Accepted for publication in ApJ Letters
Preprint typeset using LaTeX style emulateapj v. 5/2/11

THE IDENTIFICATION OF Z-DROPOUTS IN PAN-STARRS1: THREE QUASARS AT $6.5 < Z < 6.7$[1]

B. P. Venemans[2], E. Bañados[2], R. Decarli[2], E. P. Farina[2], F. Walter[2], K. C. Chambers[3], X. Fan[4], H-W. Rix[2], E. Schlafly[2], R. G. McMahon[5,6], R. Simcoe[7], D. Stern[8], W. S. Burgett[9], P. W. Draper[10], H. Flewelling[3], K. W. Hodapp[3], N. Kaiser[3], E. A. Magnier[3], N. Metcalfe[10], J. S. Morgan[3], P. A. Price[11], J. L. Tonry[3], C. Waters[3], Y. AlSayyad[12], M. Banerji[5,6], S. S. Chen[7], E. A. González-Solares[5], J. Greiner[13], C. Mazzucchelli[2], I. McGreer[4], D. R. Miller[7], S. Reed[5], P. W. Sullivan[7]

Accepted for publication in ApJ Letters

ABSTRACT

Luminous distant quasars are unique probes of the high redshift intergalactic medium (IGM) and of the growth of massive galaxies and black holes in the early universe. Absorption due to neutral Hydrogen in the IGM makes quasars beyond a redshift of $z \simeq 6.5$ very faint in the optical z-band, thus locating quasars at higher redshifts require large surveys that are sensitive above 1 micron. We report the discovery of three new $z > 6.5$ quasars, corresponding to an age of the universe of < 850 Myr, selected as z-band dropouts in the Pan-STARRS1 survey. This increases the number of known $z > 6.5$ quasars from 4 to 7. The quasars have redshifts of $z = 6.50$, 6.52, and 6.66, and include the brightest z-dropout quasar reported to date, PSO J036.5078+03.0498 with $M_{1450} = -27.4$. We obtained near-infrared spectroscopy for the quasars and from the Mg II line we estimate that the central black holes have masses between 5×10^8 and $4 \times 10^9\,M_\odot$, and are accreting close to the Eddington limit ($L_{\rm Bol}/L_{\rm Edd} = 0.13 - 1.2$). We investigate the ionized regions around the quasars and find near zone radii of $R_{\rm NZ} = 1.5 - 5.2$ proper Mpc, confirming the trend of decreasing near zone sizes with increasing redshift found for quasars at $5.7 < z < 6.4$. By combining $R_{\rm NZ}$ of the PS1 quasars with those of $5.7 < z < 7.1$ quasars in the literature, we derive a luminosity corrected redshift evolution of $R_{\rm NZ,corrected} = (7.2 \pm 0.2) - (6.1 \pm 0.7) \times (z - 6)$ Mpc. However, the large spread in $R_{\rm NZ}$ in the new quasars implies a wide range in quasar ages and/or a large variation in the neutral Hydrogen fraction along different lines of sight.

Subject headings: cosmology: observations — galaxies: active — quasars: general — quasars: individual (PSO J036.5078+03.0498, PSO J167.6415-13.4960, PSO J338.2298+29.5089)

1. INTRODUCTION

Quasars are the most luminous non-transient objects known. Their high luminosity makes quasars ideal to probe the universe at early cosmic times. Since distant ($z \gtrsim 5.7$) luminous quasars are rare, with an estimated source density of $\sim$1 per Gpc^3 (e.g., Fan et al. 2004; Willott et al. 2010b), surveys covering a large area of the sky are required to uncover the distant quasar population. Over the last 15 years more than 70 quasars with redshifts between $5.5 < z < 6.5$ have been discovered in various surveys (e.g., Fan et al. 2006; Jiang et al. 2008; Mortlock et al. 2009; Willott et al. 2010a; Morganson et al. 2012; Bañados et al. 2014). Most of these quasars have been found by looking for sources with a large break between the optical i and z-bands (e.g., Fan et al. 2006), the so-called i-band dropouts or i-dropouts. To find quasars beyond $z \sim 6.5$ wide-field surveys with coverage beyond $\sim$1 μm are needed.

Currently, four quasars above $z > 6.5$ have been discovered in near-infrared surveys. Mortlock et al. (2011) presented a quasar at $z = 7.1$ discovered in the UK infrared Telescope Infrared Deep Sky Survey (UKIDSS; Lawrence et al. 2007), while Venemans et al. (2013) reported three quasars at $6.6 < z < 6.9$ from the Visible and Infrared Survey Telescope Kilo-Degree Infrared Galaxy (VIKING) survey. Detailed studies of these four $z > 6.5$ quasars have given insight into the properties of the universe less than a Gyr after the Big

[1] Based in part on observations collected at the European Southern Observatory, Chile, programs 179.A-2010, 092.A-0150, 093.A-0863 and 093.A-0574, and at the Centro Astronómico Hispano Alemán (CAHA) at Calar Alto, operated jointly by the Max-Planck Institut für Astronomie and the Instituto de Astrofísica de Andalucía (CSIC). This paper also includes data gathered with the 6.5 meter Magellan Telescopes located at Las Campanas Observatory, Chile, at the MMT Observatory, a joint facility of the University of Arizona and the Smithsonian Institution, and with the LBT.

[2] Max-Planck Institute for Astronomy, Königstuhl 17, 69117 Heidelberg, Germany
[3] Institute for Astronomy, University of Hawaii, 2680 Woodlawn Drive, Honolulu, HI 96822, USA
[4] Steward Observatory, The University of Arizona, 933 North Cherry Avenue, Tucson, AZ 85721-0065, USA
[5] Institute of Astronomy, University of Cambridge, Madingley Road, Cambridge, CB3 0HA, UK
[6] Kavli Institute for Cosmology, University of Cambridge, Madingley Road, Cambridge CB3 0HA, UK
[7] MIT-Kavli Center for Astrophysics and Space Research, 77 Massachusetts Avenue, Cambridge, MA 02139, USA
[8] Jet Propulsion Laboratory, California Institute of Technology, 4800 Oak Grove Drive, Mail Stop 169-221, Pasadena, CA 91109, USA
[9] GMTO Corporation, 251 S. Lake Ave., Suite 300, Pasadena, CA 91101, USA
[10] Department of Physics, Durham University, South Road, Durham DH1 3LE, UK
[11] Department of Astrophysical Sciences, Princeton University, Princeton, NJ 08544, USA
[12] Department of Astronomy, University of Washington, Box 351580, Seattle, WA 98195, USA
[13] Max-Planck-Institut für extraterrestrische Physik, Giessenbachstrasse 1, 85748 Garching, Germany

Bang. For example, the optical spectrum of the $z = 7.1$ quasar places constraints on the fraction of neutral Hydrogen (Mortlock et al. 2011; Bolton et al. 2011), while Simcoe et al. (2012) uses near-infrared spectroscopy to put limits on the metal enrichment ("metallicity") of the intergalactic medium up to $z \sim 7$. Furthermore, these quasars set a lower limit to the number density of supermassive black holes at $z > 6.5$: $\rho(M_{\rm BH} > 10^9\,M_\odot) > 1.1 \times 10^{-9}\,{\rm Mpc}^{-3}$ (Venemans et al. 2013; De Rosa et al. 2014).

The limitation of both UKIDSS and VIKING is that they cover only small fractions of the extragalactic sky: UKIDSS has imaged $\sim$4000 deg^2, while VIKING will cover an area of 1500 deg^2. Overcoming this limitation, the Panoramic Survey Telescope & Rapid Response System 1 (Pan-STARRS1, PS1; Kaiser et al. 2002, 2010) has imaged the whole sky above a declination of –30° for about four years in five filters ($g_{\rm P1}$, $r_{\rm P1}$, $i_{\rm P1}$, $z_{\rm P1}$, and $y_{\rm P1}$; Stubbs et al. 2010; Tonry et al. 2012). The inclusion of the $y_{\rm P1}$ filter (central wavelength $\lambda_c = 9620$ Å, FWHM = 890 Å; Tonry et al. 2012) enables the search for luminous quasars at $z > 6.5$ over more than 20,000 deg^2 of extragalactic sky by selecting sources with a red $z_{\rm P1}$–$y_{\rm P1}$ colors (z-dropouts, see Fig. 1). In this paper we present the first results from our ongoing search for $z > 6.5$ quasars in the PS1 data.

All magnitudes are given in the AB system and we adopt a cosmology with $H_0 = 70$ km s^{-1} Mpc^{-1}, $\Omega_M = 0.28$ and $\Omega_\lambda = 0.72$ (Komatsu et al. 2011).

2. CANDIDATE SELECTION

2.1. *The Pan-STARRS1 3π Survey*

To search for z-dropouts, we made use of the first internal release of stacked PS1 imaging data (PV1). We selected our initial $z > 6.5$ quasar candidates as objects with a signal-to-noise ratio $({\rm S/N})_{y{\rm P1}} > 7$, and a non-detection in the $g_{\rm P1}$ $r_{\rm P1}$ and $i_{\rm P1}$ bands (i.e. S/N < 3). We further required a break between the $z_{\rm P1}$ and $y_{\rm P1}$ bands (see also Fig. 1 in Bañados et al. 2014):

$$({\rm S/N})_{z{\rm P1}} > 3 \text{ AND } (z_{\rm P1} - y_{\rm P1} > 1.4) \quad \text{OR}$$

$$({\rm S/N})_{z{\rm P1}} < 3 \text{ AND } (z_{\rm P1,lim,3\sigma} - y_{\rm P1} > 1.4).$$

To avoid extended sources we demanded that the difference between the $y_{\rm P1}$-band PSF and aperture magnitudes ($y_{\rm ext}$) to be consistent within 0.3 mag. This value was determined by comparing $y_{\rm ext}$ with spectroscopically confirmed stars and galaxies from the SDSS-III database[14]. Setting $y_{\rm ext} < 0.3$ selected the vast majority of stars (> 85%), while rejecting a large fraction (>94%) of galaxies. Lastly, we removed sources that were marked as likely spurious in the catalogs (see Bañados et al. 2014) or that had less than 85% of the expected flux in the $z_{\rm P1}$ or $y_{\rm P1}$ images on valid pixels. For bright sources ($y_{\rm P1} < 19.5$) we applied the same criteria but we relaxed our limits in the $g_{\rm P1}$, $r_{\rm P1}$, and $i_{\rm P1}$-bands, requiring S/N < 5.

The total number of z-dropouts selected from the PS1 catalogs after removing objects in the plane of the Milky Way and M31 ($|b| < 20°$ and $7° <$ R.A. $< 14°$; $37° <$ Decl. $< 43°$) was 328,372 (of which 13,093 had $y_{\rm P1} < 19.5$).

2.2. *Public infrared surveys*

To extend and verify the photometry of the quasar candidates selected from the PS1 catalogs we first matched the sources with several public infrared surveys.

UKIDSS: The PS1 candidates were matched with the near-infrared data of the UKIDSS survey (Lawrence et al. 2007). The UKIDSS Large Area Survey (LAS) provides Y, J, H and K imaging over $\sim$4000 deg^2. We matched the PS1 z-dropout list with the catalogs from the UKIDSS data release[15] 10, using a search radius of 2.″0. We identified objects as foreground interlopers if they had a $Y - J > 0.6$ or $y_{\rm P1} - J > 1$ (which is typical for cool dwarfs; see e.g., Best et al. 2013) and removed them from our candidate lists.

VHS: For objects in the area $150° <$ R.A. $< 240°$ and $-20° <$ Decl. $< 0°$, aperture photometry was performed on the Y, J, H and K_s images of the VISTA Hemisphere Survey (VHS; McMahon et al. 2013). We applied the same color criteria as for our UKIDSS matched list.

WISE: The *Wide-field Infrared Survey Explorer* (*WISE*; Wright et al. 2010) surveyed the entire mid-infrared sky in four bands centered at 3.4, 4.6, 12 and 22 μm. The NEOWISE observations (Mainzer et al. 2011) surveyed 70% of the sky at 3.4 and 4.6 μm (hereafter W1 and W2). Both surveys were combined to produce the AllWISE catalogs[16]. To rule out spurious candidates, we required PS1 z-dropouts without a match in the VHS or UKIDSS surveys to have a counterpart in the AllWISE catalogs within 3.″0 to be considered real sources.

Objects with a S/N > 3 in W1 and W2 were assigned a higher priority if their colors fulfilled the additional criteria: $-0.2 < W_{1,\rm AB} - W_{2,\rm AB} < 0.86$ AND $W_{1,\rm AB} - W_{2,\rm AB} > -1.45 \times (y_{\rm P1} - W_{1,\rm AB}) - 0.455$, which is loosely based on the PS1-*WISE* colors of brown dwarfs (e.g., Best et al. 2013). Objects with a S/N < 3 in W1 or W2 were assigned with an intermediate priority and the remaining candidates were given a low priority.

For the approximately 13,000 objects with a match in at least one of the above surveys, we performed forced photometry on the PS1 images to confirm the colors and non-detections (see Bañados et al. 2014). After visually inspecting the remaining $\sim$1000 candidates we selected the best $\sim$500 objects that were our main targets for follow-up observations.

3. FOLLOW-UP OBSERVATIONS

To confirm the colors of the possible quasars and to remove lower redshift interlopers, we imaged 194 z-dropout candidates during five observing runs. We obtained optical and infrared images between 2014 January 24 and 2014 August 13 with the MPG 2.2m/GROND (Greiner et al. 2008), NTT/EFOSC2 (Buzzoni et al. 1984), NTT/SofI (Moorwood et al. 1998) and the Calar Alto 3.5m/Omega2000 (Bailer-Jones et al. 2000), see Table 1 for the details of the observations.

Candidates were considered foreground interlopers if they had $y_{\rm P1} - J > 1$ (see Sect. 2.2). Sources with a

[14] http://www.sdss3.org/

[15] http://surveys.roe.ac.uk/wsa/dr10plus_release.html

[16] http://wise2.ipac.caltech.edu/docs/release/allwise/

Table 1
Imaging and Spectroscopic Observations of Quasar Candidates

Object[a]	Date	Telescope/Instrument	λ range / filters	Exposure Time	Slit Width
	2014 January 24–February 5	MPG 2.2m/GROND	g', r', i', z', J, H, K	460 s–960 s	–
	2014 March 2–6	NTT/EFOSC2	I_N, Z_N	600 s	–
	2014 March 2 & 5	NTT/SofI	J	300 s	–
	2014 March 16–19	CAHA 3.5m/Omega2000	z, Y, J	300 s–600 s	–
	2014 July 23–28	NTT/EFOSC2	I_N, Z_N	600 s	–
	2014 July 25	NTT/SofI	J	600 s	–
	2014 August 7 & 11–13	CAHA 3.5m/Omega2000	Y, J	600 s	–
P167–13	2014 April 26	VLT/FORS2	0.74–1.07 μm	2630 s	1.″3
	2014 May 30–June 2	Magellan/FIRE	0.82–2.49 μm	12004 s	0.″6
P036+03	2014 July 25	NTT/EFOSC2	0.60–1.03 μm	7200 s	1.″2
	2014 September 4–6	Magellan/FIRE	0.82–2.49 μm	8433 s	0.″6
	2014 October 20	Keck I/LRIS	0.55–1.03 μm	1800 s[b]	1.″0
P338+29	2014 October 19	MMT/Red Channel	0.67–1.03 μm	1800 s	1.″0
	2014 October 30	Magellan/FIRE	0.82–2.49 μm	7200 s[b]	0.″6
	2014 November 27	LBT/MODS	0.51–1.06 μm	2700 s	1.″2
	2014 December 6	LBT/LUCI	2.05–2.37 μm	3360 s	1.″5

[a] For the full name and coordinates, see Table 2.
[b] Observations in cloudy conditions.

$y_{\rm P1} - J < -1$ or undetected in J were rejected on the basis that they could be moving, varying or a spurious object in the PS1 catalog. We reobserved objects with $-1.0 < y_{\rm P1} - J < 1.0$ with the NTT in the filters I_N and Z_N. Only three sources remained undetected in I_N or were red with $I_N - Z_N \gtrsim 2$. These objects were targets for spectroscopy.

We obtained optical and near-infrared spectroscopy of all the three candidates that had good quasar colors after the follow-up imaging. We carried out spectroscopic observations between 2014 April 26 and 2014 December 6 using the following instruments: VLT/FORS2 (Appenzeller et al. 1998); Megallan/FIRE (Simcoe et al. 2008, 2010); NTT/EFOSC2; Keck/LRIS (Oke et al. 1995); MMT/Red Channel Spectrograph; and LBT/MODS (Pogge et al. 2010) and LBT/LUCI (Seifert et al. 2003). Details of the observations are listed in Table 1.

We reduced the data following standard reduction steps (e.g., Venemans et al. 2013; Bañados et al. 2014). We show the merged spectra in Fig. 1.

4. THREE QUASARS AT $Z > 6.5$

All three z-dropouts for which we obtained optical spectroscopy showed a strong continuum break in their optical spectrum (Fig. 1) and were identified as quasars at redshifts $6.5 < z < 6.7$. We fitted the continuum with three components: a power-law with slope β ($f_\lambda \sim \lambda^\beta$), a Balmer continuum and an Fe II template (see e.g., De Rosa et al. 2014). In all cases the Balmer continuum was found to be negligible at the wavelengths we considered ($\lambda_{\rm rest} \lesssim 3000$ Å). A single-Gaussian fit of the emission lines (most prominently C IV and Mg II) provided a sufficiently good model of the line profiles given the S/N of our spectra. Only in the spectrum of the brightest quasar, PSO J036.5078+03.0498, we were able to constrain on the Fe II emission (Section 4.2). The near-infrared spectra of the other two quasars did not have sufficient S/N. This did not significantly affect the fit of the Mg II lines in these quasars.

The redshifts were determined by the peak of the Mg II line. Other bright emission lines, such as Si IV λ 1397 and C IV λ 1549, are blueshifted by 300–2000 km s^{-1} with respect to Mg II. Such shifts are similar to those measured in spectra of other distant luminous quasars (e.g., Richards et al. 2002; De Rosa et al. 2014).

We estimated black hole masses using the local scaling relation based on the Mg II line (Eq. 1 in Vestergaard & Osmer 2009), which has a systematic uncertainty of a factor ∼3. The black hole mass uncertainties quoted in Sections 4.1–4.3 and in Table 2 represent only statistical errors.

We computed bolometric luminosities by applying the bolometric correction obtainted by Shen et al. (2008) to the monochromatic luminosity density measured at 3000 Å. The Eddington luminosity is defined as $L_{\rm Edd} = 1.3 \times 10^{38}\,(M_{\rm BH}/M_\odot)\,{\rm erg\,s^{-1}}$.

A summary of the photometric properties and the parameters derived from the spectra is provided in Table 2. Below we describe the new quasars in more detail.

4.1. *PSO J167.6415–13.4960*

The quasar PSO J167.6415–13.4960 (hereafter P167–13) was discovered based on forced photometry on VHS images at the positions of PS1 candidates. Our FORS2 discovery spectrum revealed a source with a strong continuum decrement around 9100 Å, and we identified the object as a quasar with a redshift of $z \sim 6.52$. From the near-infrared spectrum we derive a redshift $z_{\rm MgII} = 6.508 \pm 0.001$. This quasar is the faintest of our new discoveries with $M_{1450} = -25.58 \pm 0.13$. The power-law slope of $\beta = -1.0 \pm 0.1$ is red compared to the slope of $\beta = -1.3$ of the SDSS quasar composite spectrum of Vanden Berk et al. (2001). The estimated black hole mass is $M_{\rm BH,MgII} \approx (4.9 \pm 2.0) \times 10^8\,M_\odot$, and the Eddington ratio is consistent with maximal accretion ($L_{\rm Bol}/L_{\rm Edd} = 1.2 \pm 0.5$).

4.2. *PSO J036.5078+03.0498*

PSO J036.5078+03.0498 (hereafter P036+03) was selected as part of our extended, bright z-dropout search and was matched to a source in the UKIDSS and *WISE* catalogs. The high S/N FIRE spectrum revealed blue quasar continuum emission ($\beta = -1.70 \pm 0.05$) at a redshift $z_{\rm MgII} = 6.527 \pm 0.002$. The absolute magnitude of

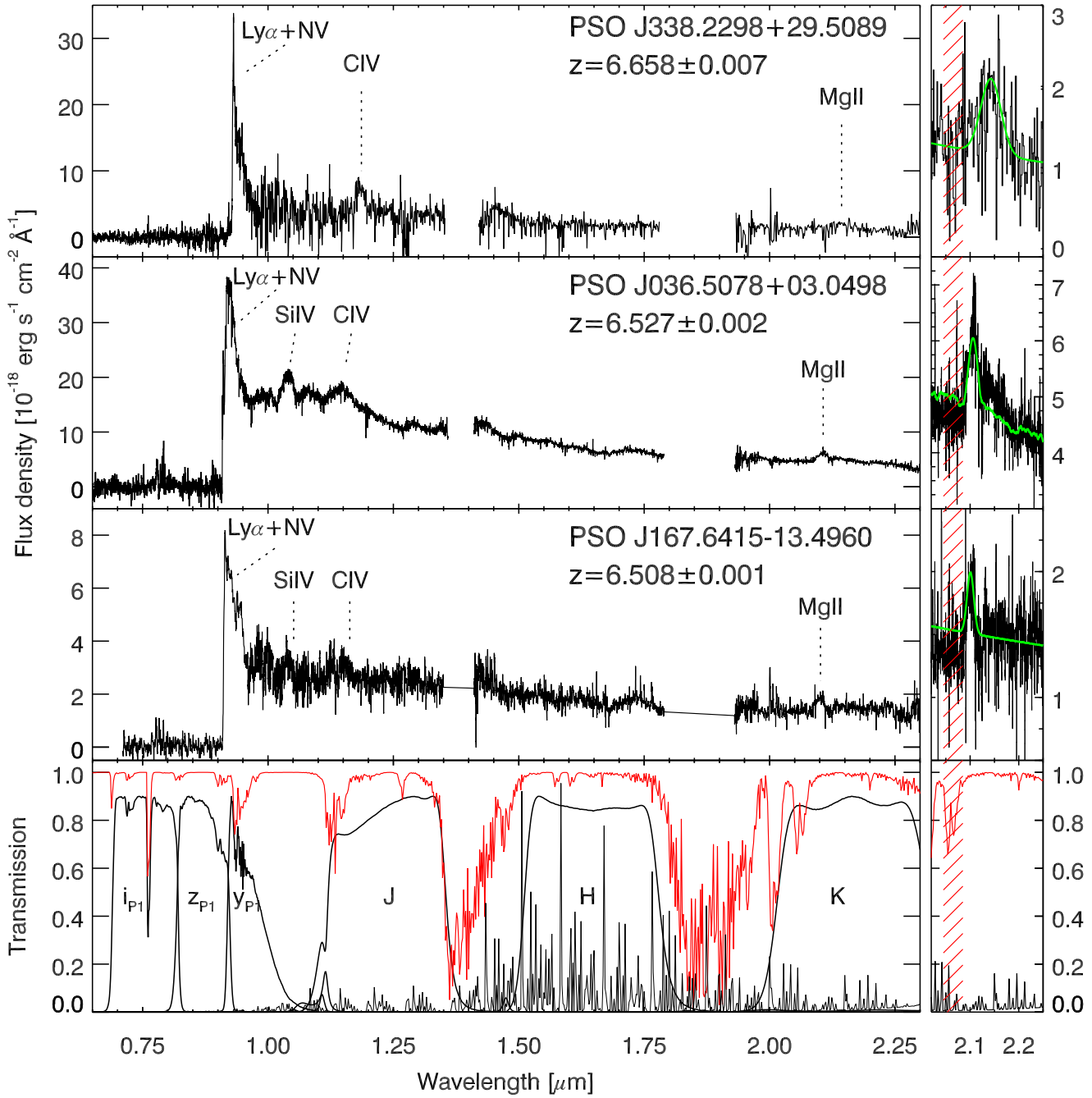

Figure 1. Merged optical and near-infrared spectra of the three new $z > 6.5$ quasars. The position of various strong, broad emission lines are indicated. The bottom panel shows the transmission curves of the $i_{\rm P1}$, $z_{\rm P1}$, and $y_{\rm P1}$ filters, and the GROND J, H and K filters. Also plotted is the relative strength of the sky emission (in black) and the telluric absorption spectrum (in red). The panels to the right show a zoom on the Mg II line with the model best fitting the line and continuum overplotted in green. The red stripes mark a region with low sky transparency that was excluded from the fitting.

$M_{1450} = -27.36 \pm 0.03$ makes this quasar one of the most luminous objects known at $z > 6$. The bolometric luminosity is estimated to be $L_{\rm Bol,3000\,\AA} = (2.38 \pm 0.09) \times 10^{47}\,{\rm erg\,s^{-1}}$. The central black hole has an estimated mass of $M_{\rm BH,MgII} = (1.9^{+1.1}_{-0.8}) \times 10^9\,M_\odot$. The accretion rate is close to Eddington with $L_{\rm Bol}/L_{\rm Edd} = 0.96 \pm 0.55$. The quality of the infrared spectrum is not sufficient to constrain the Fe II emission to better than 2σ. We measure Fe II/Mg II$= 3.4 \pm 1.7$, fully consistent with previously discovered quasars at similar redshifts (e.g., De Rosa et al. 2014).

4.3. *PSO J338.2298+29.5089*

PSO J338.2298+29.5089 (hereafter P338+29) was one of the z-dropout candidates with a match in the *WISE* catalog. The discovery spectrum shows a source with a strong, narrow emission line at ∼9314 Å and continuum redward of the line, which we identify as Lyα at a redshift of $z = 6.66$. From the FIRE spectrum we measure $z_{\rm MgII} = 6.658 \pm 0.007$, $M_{1450} = -26.04 \pm 0.09$, and a blue

Table 2
Photometric Properties and Derived Parameters of the New $z > 6.5$ Quasars From PS1.

	PSO J167.6415–13.4960	PSO J036.5078+03.0498	PSO J338.2298+29.5089
Abbreviated name	P167–13	P036+03	P338+29
R.A. (J2000)	$11^h10^m33\overset{s}{.}98$	$02^h26^m01\overset{s}{.}88$	$22^h32^m55\overset{s}{.}15$
Decl. (J2000)	$-13°29'45\overset{''}{.}6$	$+03°02'59\overset{''}{.}4$	$+29°30'32\overset{''}{.}2$
I_N	>24.68[a]	23.62 ± 0.18	>24.37[a]
$z_{\rm P1}$	>22.54[a]	21.51 ± 0.24	>22.25[a]
Z_N	22.08 ± 0.09	20.46 ± 0.04	21.92 ± 0.09
$y_{\rm P1}$	20.49 ± 0.12	19.37 ± 0.04	20.13 ± 0.08
J	21.21 ± 0.09	19.51 ± 0.03	20.74 ± 0.09
$W_{1,\rm AB}$	21.13 ± 0.39[b]	19.43 ± 0.08	20.51 ± 0.21
M_{1450}	-25.58 ± 0.13	-27.36 ± 0.03	-26.04 ± 0.09
β	-1.0 ± 0.1	-1.70 ± 0.05	$-1.85^{+0.08}_{-0.05}$
$z_{\rm MgII}$	6.508 ± 0.001	6.527 ± 0.002	6.658 ± 0.007
FWHM$_{\rm MgII}$ (km s^{-1})	2350 ± 470	3500^{+1010}_{-740}	6800^{+1200}_{-900}
$M_{\rm BH}$ ($M_\odot$)	$(4.9 \pm 2.0) \times 10^8$	$(1.9^{+1.1}_{-0.8}) \times 10^9$	$(3.7^{+1.3}_{-1.0}) \times 10^9$
$L_{\rm Bol,3000\,\AA}/L_{\rm Edd}$	1.2 ± 0.5	$0.96^{+0.70}_{-0.35}$	$0.13^{+0.05}_{-0.04}$
$R_{\rm NZ}$ (proper Mpc)	1.5 ± 0.7	3.1 ± 0.7	5.2 ± 0.7
$R_{\rm NZ,corrected}$ (proper Mpc)	2.3 ± 1.1	2.8 ± 0.6	6.9 ± 0.9

[a] Non-detections listed as 3σ upper limits.
[b] Listed in the AllWISE Reject table.

continuum slope $\beta = -1.85^{+0.08}_{-0.05}$. Although the Mg II line suffers from sky residuals on its blue side, we estimate a black hole mass of $M_{\rm BH,MgII} = (3.7^{+1.3}_{-1.0}) \times 10^9\,M_\odot$ and an accretion rate of $L_{\rm Bol}/L_{\rm Edd} = 0.13^{+0.05}_{-0.04}$.

5. QUASAR IONIZATION REGION

Quasar near zones are the regions surrounding distant quasars where the UV radiation of the central source has ionized the H I. The size of the near zone ($R_{\rm NZ}$) is a function of, among others, the quasar age, the flux of ionizing photons and the fraction of neutral H ($f_{\rm HI}$) in the IGM. A study of near zones of $5.7 < z < 6.4$ quasars was performed by Carilli et al. (2010), measuring $R_{\rm NZ}$ around 27 quasars. To compare the near zone sizes as function of redshifts, Carilli et al. (2010) scaled the measured $R_{\rm NZ}$ to an absolute magnitude of $M_{1450} = -27$: $R_{\rm NZ,corrected} = R_{\rm NZ} \times 10^{0.4(27+M1450)/3}$. They found that the ionized region around quasars decreases with increasing redshift and follows the relation $R_{\rm NZ,corrected} = (7.4 \pm 0.3) - (8.0 \pm 1.1) \times (z-6)$. This signals an increase in $f_{\rm HI}$ close to quasars at higher redshifts, although it is not straightforward to translate a change in $R_{\rm NZ}$ to a change in $f_{\rm HI}$ (e.g., Bolton & Haehnelt 2007).

We measured the near zones following the method described in Fan et al. (2006) and also employed by Carilli et al. (2010). The results are shown in Fig. 2a. We derive near zone radii of 1.5, 3.1, and 5.2 Mpc (proper) for P167–13, P036+03, and P338+29, respectively. The uncertainty in the computed near zone (including the uncertainty in the quasar's systemic redshift derived from Mg II) is about 0.7 Mpc (Carilli et al. 2010). The sizes scaled to $M_{1450} = -27$ are $R_{\rm NZ,corrected} = 2.3$, 2.8, and 6.9 Mpc, respectively.

In Fig. 2b we compare the near zones of the PS1 quasars with those of $5.7 < z < 7.1$ quasars from the literature. The PS1 quasars roughly follow the trend of smaller near zones at higher redshifts. A weighted linear fit results in a relation $R_{\rm NZ,corrected} = (7.2 \pm 0.2) - (6.1 \pm 0.7) \times (z-6)$ Mpc. Interpreting the decrease in $R_{\rm NZ}$ as an increase in $f_{\rm HI}$, $R_{\rm NZ} \propto (1+z)^{-1} f_{\rm HI}^{-1/3}$ (e.g., Fan et al. 2006, but see Bolton & Haehnelt 2007), the decrease in $R_{\rm NZ,corrected}$ by a factor 6.5 between $z = 6$ and $z = 7$ implies an increase in the neutral fraction of a factor ∼180. Combined with a measured $f_{\rm HI} \approx 2 \times 10^{-4}$ at $z \sim 6$ (e.g., Fan et al. 2006), this suggests $f_{\rm HI} \approx 0.04$ at $z = 7$, confirming the rapid evolution of $f_{\rm HI}$ at $z > 6$ (e.g., Fan et al. 2006; Bolton et al. 2011). The large spread (a factor ∼3) in (corrected) near zone sizes between individual quasars indicates a wide range in quasar ages and/or a large variation in $f_{\rm HI}$ along different lines of sight.

6. SUMMARY

We identified three new quasars at redshifts $6.5 < z < 6.7$ in PS1, nearly doubling the number of known $z > 6.5$ quasars from 4 to 7. The newly discovered quasars have a wide range of properties (Table 2). The rest-frame UV luminosities are between $M_{1450} = -25.6$ and $M_{1450} = -27.4$. The brightest of the PS1 quasars is the most luminous quasar discovered at $z > 6.5$ so far (Fig. 3), with a luminosity at 1450 Å close to that of the bright SDSS quasar J1148+5251 at $z = 6.42$ (Fan et al. 2003). The faintest PS1 quasar is only marginally brighter than the faintest $z > 6.5$ quasar found in the VIKING survey (J0109–3047; Venemans et al. 2013). Since the areal coverage of PS1 is more than 10× larger than that of VIKING, this is very promising for our continuing PS1 z-dropout search.

The PS1 quasars are powered by black holes with estimated masses between $(0.5 - 4) \times 10^9\,M_\odot$, based on the Mg II line widths and the quasar luminosities. The black holes are accreting in the range 0.13–1.2 times the Eddington limit. Black hole masses, accretion rates and (when estimated) Mg II/Fe II ratio are similar to those derived for other $z > 6$ quasars (e.g., Willott et al. 2010a; De Rosa et al. 2014).

We derived the ionized region around the quasars and found (luminosity corrected) near zones between 2.3 and 6.9 Mpc, in line with the sizes measured around $5.7 < z < 6.4$ quasars. By comparing the near zone radii of quasars between $5.7 < z < 7.1$, we derive that the av-

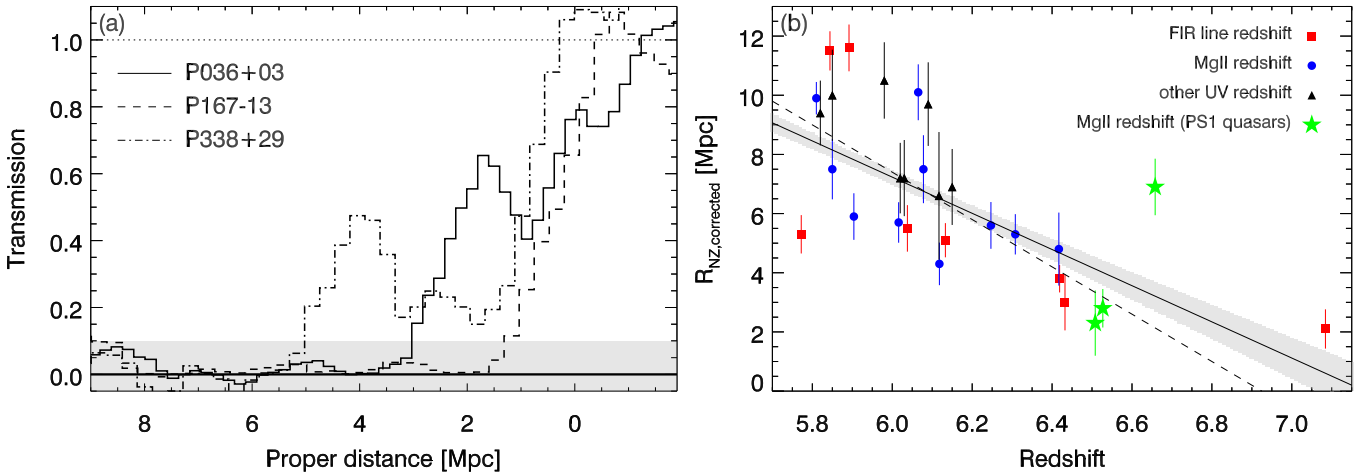

Figure 2. (a) The near zone of the quasars in physical (proper) Mpc. The transmission was computed by normalizing the observed spectra with a power-law continuum and two Gaussians fitted to the Lyα and N V lines. The resulting normalized spectra were subsequently smoothed to a resolution of 20 Å. The redshifted position of the Lyα line, based on the Mg II redshift, is taken as zeropoint on the x-axis. The grey region indicates <10% transmission. The ionized region around P167–13 extends to only ∼1.5 Mpc, while the near zones of P036+03 and P338+29 are 3.1 Mpc and 5.2 Mpc, respectively. (b) Luminosity corrected near zone radii as function of redshift for $z > 5.7$ quasars. Red squares, blue circles and black triangles represent measurements taken from Mortlock et al. (2009), Carilli et al. (2010), Willott et al. (2010a), and Mortlock et al. (2011), and were updated when more accurate redshifts have become available (Willott et al. 2010a; Venemans et al. 2012; Willott et al. 2013; Wang et al. 2013). The green stars illustrate the near zone radii of the PS1 $z > 6.5$ presented here. The black line and shaded region shows the weighted linear fit of $R_{\rm NZ,corrected} = (7.2 \pm 0.2) - (6.1 \pm 0.7) \times (z - 6)$. The dashes line show the weighted fit derived by Carilli et al. (2010) for quasars at $z \lesssim 6.4$.

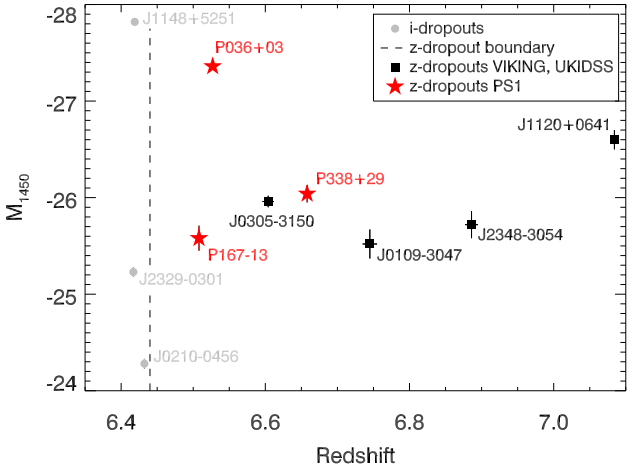

Figure 3. Absolute UV magnitude (M_{1450}) as function of redshift for all known quasars at $z > 6.4$. The dashed line indicates the minimum redshift probed by the z-dropout technique (Venemans et al. 2013). The black squares are previously known z-dropouts from Mortlock et al. (2011) and Venemans et al. (2013). The grey circles represent the highest redshift quasars discovered in optical surveys (Fan et al. 2003; Willott et al. 2007, 2010a). The new $z > 6.5$ quasars presented in this work are indicated with red stars.

erage size of the quasar ionization region decreases by a factor ∼6.5 between $z = 6$ and $z = 7$. This implies a neutral Hydrogen fraction in the IGM of a few percent at $z = 7$, although the scatter in $R_{\rm NZ}$ at all redshifts (a factor 3 between the new quasars) suggest large variations in $f_{\rm HI}$ along different lines of sight.

We thank the referee for carefully reading the manuscript and proving constructive comments and suggestions.

B.P.V., E.P.F., and F.W. acknowledge funding through ERC grant "Cosmic Dawn". E.B. thanks the IMPRS for Astronomy & Cosmic Physics at the University of Heidelberg. X.F. and I.D.M. acknowledge support from US NSF grant AST 11-07682, and R.S. and D.M. from US NSF grant AST-1109915.

The Pan-STARRS1 Surveys have been made possible through contributions of the Institute for Astronomy, University of Hawaii, the Pan-STARRS Project Office, the Max-Planck Society and its participating institutes, Max-Planck-Institute for Astronomy, Heidelberg and Max-Planck-Institute for Extraterrestrial Physics, Garching, The Johns Hopkins University, Durham University, University of Edinburgh, Queens University Belfast, Harvard-Smithsonian Center for Astrophysics, the Las Cumbres Observatory Global Telescope Network Incorporated, the National Central University of Taiwan, the Space Telescope Science Institute, the National Aeronautics and Space Administration under grant No. NNX08AR22G issued through the Planetary Science Division of the NASA Science Mission Directorate, the National Science Foundation under grant AST-1238877, the University of Maryland, and Eotvos Lorand University (ELTE).

Part of the funding for GROND was granted from the Leibniz-Prize to Prof. G. Hasinger (DFG grant HA 1850/28-1).

This publication makes use of data products from the *Wide-field Infrared Survey Explorer*, a joint project of the University of California, Los Angeles, and the Jet Propulsion Laboratory/California Institute of Technology, funded by the National Aeronautics and Space Administration.

The LBT is an international collaboration among institutions in the USA, Italy, and Germany. The partners are: The University of Arizona; Istituto Nazionale di Astrofisica, Italy; LBT Beteiligungsgesellschaft, Germany, representing the Max-Planck Society, the Astrophysical Institute Potsdam, and Heidelberg University; The Ohio State University; The Research Corporation, on behalf of

The University of Notre Dame, University of Minnesota and University of Virginia.

Facilities: PS1 (GPC1), UKIRT (WFCAM), ESO:VISTA (VIRCAM), WISE, NTT (EFOSC2, SOFI), Max Planck:2.2m (GROND), CAO:3.5m (OMEGA2000), VLT:Antu (FORS2), Magellan:Baade (FIRE), Keck:I (LRIS), MMT (Red Channel Spectrograph), LBT (MODS, LUCI).

REFERENCES

Appenzeller, I., Fricke, K., Fürtig, W., et al. 1998, Msngr, 94, 1
Bañados, E., Venemans, B. P., Morganson, E., et al. 2014, AJ, 148, 14
Bailer-Jones, C. A., Bizenberger, P., & Storz, C. 2000, Proc. SPIE, 4008, 1305
Best, W. M. J., Liu, M. C., Magnier, E. A., et al. 2013, ApJ, 777, 84
Bolton, J. S. & Haehnelt, M. G. 2007, MNRAS, 381, L35
Bolton, J. S., Haehnelt, M. G., Warren, S. J., et al. 2011, MNRAS, 416, L70
Buzzoni, B., Delabre, B., Dekker, H., et al. 1984, Msngr, 38, 9
Carilli, C. L., Wang, R., Fan, X., et al. 2010, ApJ, 714, 834
De Rosa, G., Venemans, B. P., Decarli, R., et al. 2014, ApJ, 790, 145
Fan, X., Hennawi, J. F., Richards, G. T., et al. 2004, AJ, 128, 515
Fan, X., Strauss, M. A., Becker, R. H., et al. 2006, AJ, 132, 117
Fan, X., Strauss, M. A., Schneider, D. P., et al. 2003, AJ, 125, 1649
Greiner, J., Bornemann, W., Clemens, C., et al. 2008, PASP, 120, 405
Jiang, L., Fan, X., Annis, J., et al. 2008, AJ, 135, 1057
Kaiser, N., Aussel, H., Burke, B. E., et al. 2002, Proc. SPIE, 4836, 154
Kaiser, N., Burgett, W., Chambers, K., et al. 2010, Proc. SPIE, 7733, 12
Komatsu, E., Smith, K. M., Dunkley, J., et al. 2011, ApJS, 192, 18
Lawrence, A., Warren, S. J., Almaini, O., et al. 2007, MNRAS, 379, 1599
Mainzer, A., Bauer, J., Grav, T., et al. 2011, ApJ, 731, 53
McMahon, R. G., Banerji, M., Gonzalez, E., et al. 2013, Msngr, 154, 35
Moorwood, A., Cuby, J.-G., & Lidman, C. 1998, Msngr, 91, 9
Morganson, E., De Rosa, G., Decarli, R., et al. 2012, AJ, 143, 142
Mortlock, D. J., Patel, M., Warren, S. J., et al. 2009, A&A, 505, 97
Mortlock, D. J., Warren, S. J., Venemans, B. P., et al. 2011, Natur, 474, 616
Oke, J. B., Cohen, J. G., Carr, et al. 1995, PASP, 107, 375
Pogge, R. W., Atwood, B., Brewer, D. F., et al. 2010, Proc. SPIE, 7735, 9
Richards, G. T., Vanden Berk, D. E., Reichard, T. A., et al. 2002, AJ, 124, 1
Seifert, W., Appenzeller, I., Baumeister, H., et al. 2003, Proc. SPIE, 4841, 962
Shen, Y., Greene, J. E., Strauss, M. A., Richards, G. T., & Schneider, D. P. 2008, ApJ, 680, 169
Simcoe, R. A., Burgasser, A. J., Bernstein, R. A., et al. 2008, Proc. SPIE, 7014, 70140U
Simcoe, R. A., Burgasser, A. J., Bochanski, J. J., et al. 2010, Proc. SPIE, 7735, 772514
Simcoe, R. A., Sullivan, P. W., Cooksey, K. L., et al. 2012, Natur, 492, 79
Stubbs, C. W., Doherty, P., Cramer, C., et al. 2010, ApJS, 191, 376
Tonry, J. L., Stubbs, C. W., Lykke, K. R., et al. 2012, ApJ, 750, 99
Vanden Berk, D. E., Richards, G. T., Bauer, A., et al. 2001, AJ, 122, 549
Venemans, B. P., Findlay, J. R., Sutherland, W. J., et al. 2013, ApJ, 779, 24
Venemans, B. P., McMahon, R. G., Walter, F., et al. 2012, ApJL, 751, L25
Vestergaard, M. & Osmer, P. S. 2009, ApJ, 699, 800
Wang, R., Wagg, J., Carilli, C. L., et al. 2013, ApJ, 773, 44
Willott, C. J., Albert, L., Arzoumanian, D., et al. 2010a, AJ, 140, 546
Willott, C. J., Delorme, P., Omont, A., et al. 2007, AJ, 134, 2435
Willott, C. J., Delorme, P., Reylé, C., et al. 2010b, AJ, 139, 906
Willott, C. J., Omont, A., & Bergeron, J. 2013, ApJ, 770, 13
Wright, E. L., Eisenhardt, P. R. M., Mainzer, A. K., et al. 2010, AJ, 140, 1868